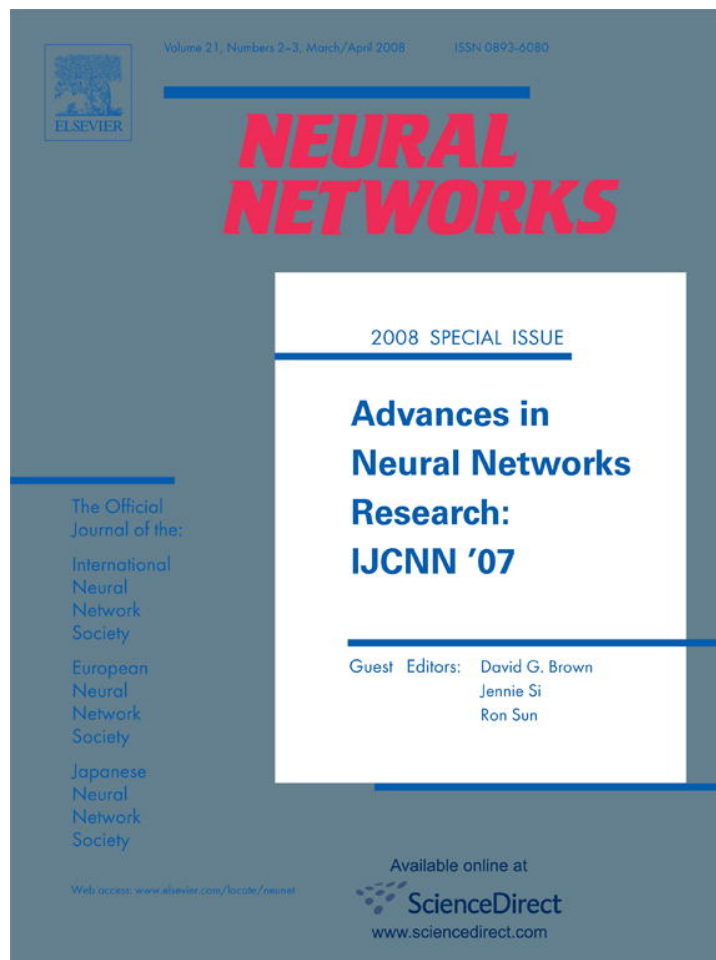


Provided for non-commercial research and education use.
Not for reproduction, distribution or commercial use.



This article was published in an Elsevier journal. The attached copy is furnished to the author for non-commercial research and education use, including for instruction at the author's institution, sharing with colleagues and providing to institution administration.

Other uses, including reproduction and distribution, or selling or licensing copies, or posting to personal, institutional or third party websites are prohibited.

In most cases authors are permitted to post their version of the article (e.g. in Word or Tex form) to their personal website or institutional repository. Authors requiring further information regarding Elsevier's archiving and manuscript policies are encouraged to visit:

<http://www.elsevier.com/copyright>



2008 Special Issue

Adaptive nonlinear least bit error-rate detection for symmetrical RBF beamforming[☆]

S. Chen^{*}, A. Wolfgang, C.J. Harris, L. Hanzo*School of Electronics and Computer Science, University of Southampton, Southampton SO17 1BJ, UK*

Received 20 July 2007; received in revised form 25 October 2007; accepted 11 December 2007

Abstract

A powerful symmetrical radial basis function (RBF) aided detector is proposed for nonlinear detection in so-called rank-deficient multiple-antenna assisted beamforming systems. By exploiting the inherent symmetry of the optimal Bayesian detection solution, the proposed RBF detector becomes capable of approaching the optimal Bayesian detection performance using channel-impaired training data. A novel nonlinear least bit error algorithm is derived for adaptive training of the symmetrical RBF detector based on a stochastic approximation to the Parzen window estimation of the detector output's probability density function. The proposed adaptive solution is capable of providing a signal-to-noise ratio gain in excess of 8 dB against the theoretical linear minimum bit error rate benchmark, when supporting four users with the aid of two receive antennas or seven users employing four receive antenna elements.

© 2007 Elsevier Ltd. All rights reserved.

Keywords: Radial basis function network; Symmetry; Probability density function; Recursive learning; Stochastic algorithm; Multiple-antenna system; Beamforming

1. Introduction

The ever-increasing demand for an improved throughput in mobile communication has motivated the development of adaptive antenna-array assisted spatial-processing techniques (Blogh & Hanzo, 2002; Godara, 1997a, 1997b; Kohno, 1998; Litva & Lo, 1996; Paulraj & Papadias, 1997; Paulraj, Nabar, & Gore, 2003; Paulraj, Gore, Nabar, & Bölcskei, 2004; Soni, Buehrer, & Benning, 2002; Tse & Viswanath, 2005; Tsoulos, 1999; Tsoulos, Beach, & McGeehan, 1997; Vandenameele, van Der Perre, & Engels, 2001; Wells, 1996; Winters, 1998; Winters, Salz, & Gitlin, 1994) in order to further improve the achievable spectral efficiency. A specific technique that has shown real promise in achieving substantial capacity enhancements is constituted by adaptive beamforming. Upon appropriately combining the signals received by the antenna

array, adaptive beamforming is capable of separating user signals transmitted on the same carrier frequency, provided that the signal sources are sufficiently separated in the angular domain. Classically, this is achieved by a linear beamformer based on the minimum mean square error (L-MMSE) solution (Blogh & Hanzo, 2002; Godara, 1997b; Litva & Lo, 1996; Paulraj et al., 2003; Soni et al., 2002; Tse & Hanly, 1999). This traditional L-MMSE beamforming design requires that the number of users supported is no more than the number of receive antenna elements. If this condition is not met, the system is referred to as overloaded or rank-deficient. The optimal solution for the linear beamforming has been shown to be the minimum bit error rate (L-MBER) design (Chen, Ahmad, & Hanzo, 2005; Chen, Hanzo, Ahmad, & Wolfgang, 2005). The L-MBER beamforming outperforms the L-MMSE one and it is capable of operating in hostile rank-deficient scenarios. It is well known, however, that digital communication signal detection in general and in multiple antenna-aided beamforming systems in particular can be viewed as a classification problem (Abend & Fritchman, 1970; Chen, McLaughlin, Mulgrew, & Grant, 1995; Chen, Hanzo, & Wolfgang, 2004b), where the receiver detector simply classifies the received multidimensional channel-impaired signal into the most likely transmitted symbol constellation point

[☆] An abbreviated version of some portions of this article appeared in Chen, Wolfgang, Harris, and Hanzo (2007) as part of the IJCNN 2007 Conference Proceedings, published under IEE copyright.

^{*} Corresponding author. Tel.: +44 (0) 23 8059 6660; fax: +44 (0) 23 8059 4508.

E-mail addresses: sqc@ecs.soton.ac.uk (S. Chen), aw03r@ecs.soton.ac.uk (A. Wolfgang), cjh@ecs.soton.ac.uk (C.J. Harris), lh@ecs.soton.ac.uk (L. Hanzo).

or class. Both radial basis function (RBF) networks (Chen & Mulgrew, 1992; Chen, Mulgrew, & Grant, 1993; Wolfgang, Chen, & Hanzo, 2004) as well as other kernel models (Albu & Martinez, 1999; Chen, Samingan, & Hanzo, 2001; Chen, Gunn, & Harris, 2001; Chen et al., 2004b; Pérez-Cruz, Navia-Vázquez, Alarcón-Diana, & Artés-Rodríguez, 2001; Sebald & Bucklew, 2000) have been applied to solve this nonlinear detection problem. All these RBF or kernel-based detectors attempt to realize or approximate the underlying optimal Bayesian solution.

The standard RBF or kernel-based modelling technique constitutes a black-box approach that seeks to extract a sparse model representation from the available training data. Adopting this black-box modelling approach is appropriate, if no *a priori* information exists regarding the underlying data generating mechanism. If, however, there exists some *a priori* information concerning the system to be modelled, a fundamental principle in practical data modelling is that the prior information should be incorporated into the modelling process. The use of prior knowledge in data modelling often leads to an improved performance. Many real-life phenomena exhibit inherent properties, such as symmetry, but these properties are often hard to infer from the data with the aid of black-box RBF or kernel models. In regression modelling, the symmetrical properties of the underlying system have been exploited by imposing symmetry in the context of both RBF networks and least squares support vector machines (Aguirre, Lopes, Amaral, & Letellier, 2004; Espinoza, Suykens, & De Moor, 2005). These two studies have shown that, by imposing symmetry on the model's structure, it is easier to extract the inherent symmetry properties of the underlying system from noisy training data and this leads to substantial improvements in the achievable regression modelling performance. We argue that it is equally important to exploit the inherent symmetry in classification applications, and hence the first novel contribution of this paper is to propose a symmetrical RBF network detector for multiple-antenna aided beamforming systems.

In fact, the work of Chen, Mulgrew, and Hanzo (2000) and Chen, Hanzo, and Mulgrew (2001) implies that the optimal Bayesian nonlinear detection solution has an inherent odd symmetry because the signal states corresponding to the different signal classes are distributed symmetrically. This inherent symmetrical property of the optimal Bayesian solution is difficult to infer from the noisy training data using standard RBF or kernel models. Previous studies (Albu & Martinez, 1999; Chen & Mulgrew, 1992; Chen et al., 1993; Chen, Samingan, et al., 2001; Chen, Gunn, et al., 2001; Chen et al., 2004b; Pérez-Cruz et al., 2001; Sebald & Bucklew, 2000; Wolfgang et al., 2004) have shown that a standard RBF or kernel detector typically requires significantly more RBF centres or kernels than the number of legitimate channel output states in order to approximate the Bayesian detector using noisy training data, and often there is a performance difference between such a kernel detector and the optimal Bayesian solution. In contrast to the standard RBF model, we will demonstrate that the proposed symmetrical RBF model is capable of approaching the optimal Bayesian performance

accurately, despite using channel-impaired training data and despite using no more RBF centres than the number of legitimate channel output states. The advantage of the proposed symmetrical RBF detector is demonstrated in challenging detection scenarios, when the number of users supported is almost twice the number of antenna array elements. Although we develop the symmetrical RBF detector in the context of multiple-antenna-aided beamforming systems, the idea is applicable in symmetrical classification problems. To the best of our knowledge, this is the first time that the symmetry is explicitly exploited in RBF or kernel classifier construction.

Most of the learning algorithms derived for training the RBF or kernel classifiers are block based. For communication detection applications, however, it is highly desirable to update the detector's parameters on a prompt sample-by-sample basis for the sake of maintaining a low real-time computational complexity as well as for ensuring that the receiver becomes capable of tracking highly time-variant channels. The second novel contribution of this paper is the introduction of a stochastic learning algorithm, referred to as the nonlinear least bit error rate (NLBER) technique, invoked for the adaptive training of the symmetrical RBF detector. We point out that the classical stochastic gradient algorithm based on the mean square error (MSE) criterion, referred to as the nonlinear least mean square (NLMS) technique, is inappropriate for the adaptive training of a nonlinear detector, since the performance metric to be optimised should be the detection error probability or bit error rate (BER). If the probability density function (PDF) of the detector's output is known analytically, the BER expression of the detector can be formulated and the detector's parameters can be tuned by directly minimizing the BER rather than the MSE. The PDF of the nonlinear detector's output, although generally unknown, can be sufficiently accurately modelled with the aid of Parzen window estimation (Bowman & Azzalini, 1997; Parzen, 1962; Silverman, 1996), which in turn gives rise to an approximate BER estimate for the nonlinear detector. By minimizing this approximate BER of the detector, an approximate nonlinear minimum BER solution is obtained. Adopting a stochastic approximation of this Parzen window-based PDF estimate leads to the proposed NLBER algorithm. The efficiency of this adaptive NLBER algorithm will be demonstrated using simulations.

The remainder of the paper is organized as follows. In Section 2 we present the beamforming signal model considered and discuss the inherent symmetrical structure of the optimal Bayesian detection solution. Based on the system model of Section 2, the novel symmetrical RBF detector is presented and the powerful adaptive NLBER algorithm is derived in Section 3. The achievable performance of this NLBER-based RBF detector is investigated in Section 4, using the optimal Bayesian solution as well as the low-complexity theoretical L-MBER beamformer as two benchmarks, while in Section 5 we offer our conclusions.

2. Multiple-antenna assisted beamforming system

We consider a coherent communication system that supports M users, where each user transmits on the same carrier

frequency of $\omega = 2\pi f$. For such a system, user separation can be achieved in the spatial or angular domain (Paulraj et al., 2003; Tse & Viswanath, 2005) and the receiver is equipped with a linear antenna array consisting of L uniformly spaced elements. We assume furthermore that the channel is nondispersive and hence it does not induce intersymbol interference. Then the symbol-rate complex-valued received signal samples can be expressed as (Blogh & Hanzo, 2002; Litva & Lo, 1996)

$$x_l(k) = \sum_{i=1}^M A_i b_i(k) e^{j\omega t_l(\theta_i)} + n_l(k) = \bar{x}_l(k) + n_l(k), \quad (1)$$

for $1 \leq l \leq L$, where $t_l(\theta_i)$ is the relative time delay at array element l for source i , with θ_i being the direction of arrival for source i , $n_l(k)$ is the complex-valued Gaussian white noise with $E[|n_l(k)|^2] = 2\sigma_n^2$, A_i is the complex-valued nondispersive channel coefficient of user i , and $b_i(k)$ is the k -th symbol of user i , which assumes values from a binary phase shift keying (BPSK) symbol set, i.e. we have $b_i(k) \in \{\pm 1\}$. Without loss of generality, source 1 is assumed to be the desired user and the rest of the sources are the interfering users. The desired user's signal-to-noise ratio (SNR) is given by $\text{SNR} = |A_1|^2 \sigma_b^2 / 2\sigma_n^2$, where $\sigma_b^2 = 1$ is the BPSK symbol energy, and the desired signal-to-interferer i ratio (SIR) is defined by $\text{SIR}_i = |A_1|^2 / |A_i|^2$, for $2 \leq i \leq M$. The received signal vector $\mathbf{x}(k) = [x_1(k) \ x_2(k) \ \dots \ x_L(k)]^T$ can be expressed as

$$\mathbf{x}(k) = \mathbf{P}\mathbf{b}(k) + \mathbf{n}(k) = \bar{\mathbf{x}}(k) + \mathbf{n}(k), \quad (2)$$

where we have $\mathbf{n}(k) = [n_1(k) \ n_2(k) \ \dots \ n_L(k)]^T$ and the system matrix \mathbf{P} is given by

$$\mathbf{P} = [A_1 \mathbf{s}_1 \ A_2 \mathbf{s}_2 \ \dots \ A_M \mathbf{s}_M] \quad (3)$$

with the steering vector of source i given by

$$\mathbf{s}_i = \left[e^{j\omega t_1(\theta_i)} \ e^{j\omega t_2(\theta_i)} \ \dots \ e^{j\omega t_L(\theta_i)} \right]^T, \quad (4)$$

and the transmitted BPSK symbol vector by $\mathbf{b}(k) = [b_1(k) \ b_2(k) \ \dots \ b_M(k)]^T$.

Although we assume a uniformly-spaced linear antenna array, the results can be extended to other antenna array structures. In fact, our discussions are applicable to the generic multiple-input multiple-output communication system (Paulraj et al., 2003; Tse & Viswanath, 2005), where the (i, j) -th element of the system matrix \mathbf{P} represents the channel coefficient connecting the j -th transmit antenna to the i -th receive antenna. Extension to the multi-level modulation schemes is also possible (Chen, Hanzo, et al., 2001, 2005; Chen, Du, & Hanzo, 2006). An assumption for the signal model (2) is that the desired user and interfering signals are symbol-synchronized. For the downlink scenario synchronous transmission of the users is guaranteed. By contrast, in an uplink scenario, the differently delayed asynchronous signals of the users are no longer automatically synchronized. However, the quasi-synchronous operation of the system may be achieved with the aid of adaptive timing advance control as in the global system of mobile (GSM) (Steele & Hanzo, 1999). The GSM system has

a timing-advance control accuracy of 0.25 bit duration. Since synchronous systems perform better than their asynchronous counterparts, the third-generation partnership research consortium (3GPP) is also considering the employment of timing-advance control in next-generation systems.

Traditionally, a linear beamforming receiver is adopted to detect the desired user's signal (Blogh & Hanzo, 2002; Litva & Lo, 1996). The output of the linear beamformer is defined by

$$y_{\text{Lin}}(k) = \boldsymbol{\alpha}^H \mathbf{x}(k) \quad (5)$$

and the associated decision is given by

$$\hat{b}_1(k) = \text{sgn}(\Re[y_{\text{Lin}}(k)]) = \begin{cases} +1, & \Re[y_{\text{Lin}}(k)] \geq 0, \\ -1, & \Re[y_{\text{Lin}}(k)] < 0, \end{cases} \quad (6)$$

where $\boldsymbol{\alpha} = [\alpha_1 \ \alpha_2 \ \dots \ \alpha_L]^T$ denotes the complex-valued linear beamformer's weight vector and $\Re[\bullet]$ the real part. Classically, the L-MMSE solution for the weight vector of the linear beamformer (5) is regarded as the optimal design (Blogh & Hanzo, 2002; Godara, 1997b; Litva & Lo, 1996; Paulraj et al., 2003; Soni et al., 2002; Tse & Hanly, 1999), and the L-MMSE beamforming can readily be implemented adaptively using the well-known least mean square (LMS) algorithm. The L-MMSE technique, apart from its noise enhancement problem, requires that the number of users M is no higher than the number of antenna array elements L . Minimizing the MSE does not guarantee minimizing the BER, and the optimal weight vector designed for the linear beamformer is known to be the L-MBER solution (Chen, Ahmad, et al., 2005), which directly minimizes the BER of the linear beamformer (5). This approach is capable of operating in rank-deficient scenarios, and adaptive implementation of the L-MBER design can be realized using the least bit error rate (LBER) algorithm (Chen, Ahmad, et al., 2005; Chen, Hanzo, et al., 2005).

However, the optimal solution for the multiple-antenna aided beamforming detector is nonlinear (Chen, Hanzo, & Wolfgang, 2004a; Chen et al., 2004b). Let us denote the $N_b = 2^M$ legitimate combinations of $\mathbf{b}(k)$ as \mathbf{b}_q , $1 \leq q \leq N_b$. Denote furthermore the first element of \mathbf{b}_q , corresponding to the desired user, as $b_{q,1}$. The noiseless channel output $\bar{\mathbf{x}}(k)$ only takes values from the finite signal state set

$$\bar{\mathbf{x}}(k) \in \mathbf{X} \triangleq \{\bar{\mathbf{x}}_q = \mathbf{P}\mathbf{b}_q, \ 1 \leq q \leq N_b\}. \quad (7)$$

The signal state set \mathbf{X} can be divided into two subsets conditioned on the value of $b_1(k)$ as follows

$$\mathbf{X}^{(\pm)} \triangleq \{\bar{\mathbf{x}}_i \in \mathbf{X}, \ 1 \leq i \leq N_{sb} : b_1(k) = \pm 1\}, \quad (8)$$

where the size of $\mathbf{X}^{(+)}$ and $\mathbf{X}^{(-)}$ is $N_{sb} = N_b/2 = 2^{M-1}$. Denote the conditional probabilities of receiving $\mathbf{x}(k)$ given $b_1(k) = \pm 1$ as $p_{\pm}(\mathbf{x}(k)) = p(\mathbf{x}(k)|b_1(k) = \pm 1)$. According to Bayes' decision theory (Duda & Hart, 1973), the optimal detection strategy should be

$$\hat{b}_1(k) = \begin{cases} +1, & \text{if } p_+(\mathbf{x}(k)) \geq p_-(\mathbf{x}(k)), \\ -1, & \text{if } p_+(\mathbf{x}(k)) < p_-(\mathbf{x}(k)). \end{cases} \quad (9)$$

If we introduce the following real-valued Bayesian decision variable

$$y_{\text{Bay}}(k) = f_{\text{Bay}}(\mathbf{x}(k)) \triangleq \frac{1}{2}p_+(\mathbf{x}(k)) - \frac{1}{2}p_-(\mathbf{x}(k)), \quad (10)$$

the optimal Bayesian detection rule (9) is equivalent to $\hat{b}_1(k) = \text{sgn}(y_{\text{Bay}}(k))$.

The decision variable (10) of the optimal Bayesian detector can be expressed as (Chen et al., 2004a, 2004b)

$$y_{\text{Bay}}(k) = \sum_{q=1}^{N_b} \text{sgn}(b_{q,1})\beta_q e^{-\frac{\|\mathbf{x}(k) - \bar{\mathbf{x}}_q\|^2}{2\sigma_n^2}} \quad (11)$$

where β_q is proportional to the *a priori* probability of $\bar{\mathbf{x}}_q$. Since in our case, all the $\bar{\mathbf{x}}_q$ are equiprobable, we have $\beta_q = \beta = \frac{1}{N_b(2\pi\sigma_n^2)^L}$. It can be readily shown that the two subsets $\mathcal{X}^{(+)}$ and $\mathcal{X}^{(-)}$ are distributed symmetrically with respect to each other (Chen et al., 2000; Chen, Hanzo, et al., 2001). Thus, when using an appropriate indexing, for any signal state $\bar{\mathbf{x}}_i^{(+)} \in \mathcal{X}^{(+)}$ there exists a signal state $\bar{\mathbf{x}}_i^{(-)} \in \mathcal{X}^{(-)}$ satisfying

$$\bar{\mathbf{x}}_i^{(-)} = -\bar{\mathbf{x}}_i^{(+)}. \quad (12)$$

Given this symmetry, the optimal Bayesian detector (11) can be characterized as

$$y_{\text{Bay}}(k) = \sum_{q=1}^{N_{sb}} \beta_q \left(e^{-\frac{\|\mathbf{x}(k) - \bar{\mathbf{x}}_q^{(+)}\|^2}{2\sigma_n^2}} - e^{-\frac{\|\mathbf{x}(k) + \bar{\mathbf{x}}_q^{(+)}\|^2}{2\sigma_n^2}} \right), \quad (13)$$

where $\bar{\mathbf{x}}_q^{(+)} \in \mathcal{X}^{(+)}$. Note that the Bayesian detector has *odd* symmetry, as $f_{\text{Bay}}(-\mathbf{x}(k)) = -f_{\text{Bay}}(\mathbf{x}(k))$.

If the system matrix \mathbf{P} of (3) is known, the signal state subset $\mathcal{X}^{(+)}$ can be computed and the Bayesian detection solution is specified. For the multiple-antenna aided beamformer in downlink, however, the receiver only has access to the training data $D_K = \{\mathbf{x}(k), b_1(k)\}_{k=1}^K$, where K is the number of training symbols and $\{b_1(k)\}$ are the desired user's data. But the receiver does not have access to the interfering users' data $\{b_i(k)\}$, $i \neq 1$. Thus, estimating the system matrix \mathbf{P} is a challenging task. In our previous work (Chen et al., 2004a, 2004b), standard RBF detectors were constructed using the channel-impaired training data set to generate RBF kernels and hence to approximate the optimal Bayesian solution. It is clear, however, that the inherent symmetry of the Bayesian detector in (13) is hard to infer from the channel-impaired data by a standard RBF detector. In this study, we propose the novel symmetrical RBF detector which renders realization of the symmetrical optimal Bayesian detection solution (13) easier.

Before formulating the symmetrical RBF detector for the BPSK modulated signals, we point out that our approach can be generalized to the general modulation scheme. This is because the ‘‘symmetry’’ properties of the channel state set \mathcal{X} for the generic modulation scheme are inherent from the symmetry of the symbol constellation. For the BPSK modulation scheme, the symmetry of the BPSK symbol constellation leads to the odd symmetry relationship of (12). For higher-order modulation schemes, the symmetry relationship of \mathcal{X} is more complicated. For example, the symmetrical properties for the quadrature phase shift keying (QPSK) signalling have been

derived by Chen, Hanzo, and Tan (submitted for publication), and these symmetrical properties are exploited in Chen et al. (submitted for publication) to form a (more sophisticated) symmetrical RBF detector for QPSK systems.

3. Symmetrical RBF detector and nonlinear least bit error algorithm

Consider the problem of training a generic RBF aided detector based on a training data set $D_K = \{\mathbf{x}(k), d(k)\}_{k=1}^K$, where $d(k) = b_1(k) \in \{1, -1\}$ denotes the class type for each complex-valued data sample $\mathbf{x}(k) \in \mathbb{C}^L$. More specifically, we consider the RBF detector of the form

$$y_{\text{RBF}}(k) = f_{\text{RBF}}(\mathbf{x}(k); \mathbf{w}) = \sum_{i=1}^{n_c} \alpha_i \phi_i(\mathbf{x}(k)), \quad (14)$$

where $f(\bullet; \bullet)$ is a real-valued nonlinear mapping realized by the RBF network, α_i is the i -th real-valued RBF weight, $\phi_i(\bullet)$ denotes the response of the i -th RBF node, n_c is the number of RBF nodes used, and \mathbf{w} denotes the vector of all the adjustable parameters of the RBF detector. The RBF detector makes the decision according to $\hat{d}(k) = \text{sgn}(y_{\text{RBF}}(k))$, where $\hat{d}(k)$ denotes the estimated class label or estimated desired symbol associated with $\mathbf{x}(k)$. In contrast to the standard RBF model, we propose to adopt the following symmetrical RBF node

$$\phi_i(\mathbf{x}) \triangleq \varphi(\mathbf{x}; \mathbf{c}_i, \sigma_i^2) - \varphi(\mathbf{x}; -\mathbf{c}_i, \sigma_i^2), \quad (15)$$

where $\mathbf{c}_i \in \mathbb{C}^L$ is the i -th complex-valued RBF centre, σ_i^2 the i -th real-valued RBF variance, and $\varphi(\bullet)$ is the classic RBF function. The parameter vector \mathbf{w} of the symmetrical RBF detector (14) therefore consists of all the real-valued RBF weights α_i , complex-valued RBF centre vectors \mathbf{c}_i as well as real-valued and positive RBF variances σ_i^2 . In this study we adopt the Gaussian RBF function of

$$\varphi(\mathbf{x}; \mathbf{c}_i, \sigma_i^2) = e^{-\frac{\|\mathbf{x} - \mathbf{c}_i\|^2}{\sigma_i^2}}. \quad (16)$$

Note that the symmetric RBF network (14) with the node structure defined in (15) has an inherently odd symmetry, just as the Bayesian detector. In the standard RBF model, by contrast, a RBF node is defined simply by $\phi_i(\mathbf{x}) \triangleq \varphi(\mathbf{x}; \mathbf{c}_i, \sigma_i^2)$, and such a RBF model cannot guarantee odd symmetry, particularly when the RBF centres are generated from the channel-impaired training data.

The block-data orientated construction algorithms (Chen et al., 2004a, 2004b), originally derived for the standard RBF detector, can also be applied here to construct the symmetrical RBF detector of (14), and this is demonstrated in the recent study (Chen et al., 2007). However, as argued in the introduction section, it is highly desirable to adaptively adjust the detector on a sample-by-sample basis. Again if the MSE criterion of $E[|d(k) - y_{\text{RBF}}(k)|^2]$ is adopted, we arrive at the nonlinear version of the well-known LMS adaptive algorithm, which we refer to as the NLMS algorithm. This NLMS algorithm can be used here for training the symmetrical

RBF detector (14)

$$\begin{cases} y_{\text{RBF}}(k) = f_{\text{RBF}}(\mathbf{x}(k); \mathbf{w}(k-1)), \\ \mathbf{w}(k) = \mathbf{w}(k-1) + \mu(d(k) - y_{\text{RBF}}(k)) \\ \quad \times \frac{\partial f_{\text{RBF}}(\mathbf{x}(k); \mathbf{w}(k-1))}{\partial \mathbf{w}}, \end{cases} \quad (17)$$

where μ is the step size. However, minimizing the MSE does not necessarily produce a low BER. It can be readily seen that multiplying the weights β_q of the optimal Bayesian detector by a positive scalar will change the MSE value of the detector, albeit the resultant detector remains the optimal Bayesian one. Similarly, multiplying the weights of the symmetric RBF detector (14) with a positive scalar will change its MSE value but not its BER. Therefore, the MSE criterion may result in a suboptimal BER performance, and hence we derive an adaptive algorithm for the nonlinear detector (14) based on an (approximate) nonlinear MBER criterion.

Let us define the following signed decision variable $y_s(k) = \text{sgn}(d(k))y_{\text{RBF}}(k)$ and denote the PDF of $y_s(k)$ as $p_y(y_s)$. Then the error probability of the nonlinear detector (14) is given by

$$P_E(\mathbf{w}) = \text{Prob}\{y_s(k) < 0\} = \int_{-\infty}^0 p_y(y_s) dy_s. \quad (18)$$

The MBER solution for the detector's parameter vector \mathbf{w} is defined as

$$\mathbf{w}_{\text{MBER}} = \arg \min_{\mathbf{w}} P_E(\mathbf{w}). \quad (19)$$

The problem associated with this approach is that the PDF of $y_s(k)$ is generally unknown. However, it may be sufficiently accurately estimated using the Parzen window method (Bowman & Azzalini, 1997; Parzen, 1962; Silverman, 1996). Given a block of training data D_K , a Parzen window estimate of $p_y(y_s)$ is readily given as

$$\tilde{p}_y(y_s) = \frac{1}{K\sqrt{2\pi}\rho} \sum_{k=1}^K e^{-\frac{(y_s - \text{sgn}(d(k))y_{\text{RBF}}(k))^2}{2\rho^2}}, \quad (20)$$

where ρ^2 is the chosen kernel variance. With this estimated PDF, the estimated or approximate BER is given by

$$\tilde{P}_E(\mathbf{w}) = \int_{-\infty}^0 \tilde{p}_y(y_s) dy_s = \frac{1}{K} \sum_{k=1}^K Q(\tilde{g}_k(\mathbf{w})), \quad (21)$$

where

$$Q(u) = \frac{1}{\sqrt{2\pi}} \int_u^{\infty} e^{-\frac{v^2}{2}} dv \quad (22)$$

and

$$\tilde{g}_k(\mathbf{w}) = \frac{\text{sgn}(d(k))y_{\text{RBF}}(k)}{\rho}. \quad (23)$$

An approximate MBER solution for \mathbf{w} can be obtained by minimizing $\tilde{P}_E(\mathbf{w})$ using a gradient-based optimization algorithm. The gradient of $\tilde{P}_E(\mathbf{w})$ is given by

$$\begin{aligned} \nabla \tilde{P}_E(\mathbf{w}) = & -\frac{1}{K\sqrt{2\pi}\rho} \sum_{k=1}^K e^{-\frac{y_{\text{RBF}}^2(k)}{2\rho^2}} \text{sgn}(d(k)) \\ & \times \frac{\partial f_{\text{RBF}}(\mathbf{x}(k); \mathbf{w})}{\partial \mathbf{w}}. \end{aligned} \quad (24)$$

The following steepest-descent gradient algorithm based on a block of training samples may be used to arrive at an approximate MBER solution

$$\begin{cases} y_{\text{RBF}}(k) = f_{\text{RBF}}(\mathbf{x}(k); \mathbf{w}(\iota-1)), & 1 \leq k \leq K, \\ \mathbf{w}(\iota) = \mathbf{w}(\iota-1) - \mu \nabla \tilde{P}_E(\mathbf{w}(\iota-1)), \end{cases} \quad (25)$$

where ι indicates the iteration index. The step size μ and kernel variance ρ^2 are the two algorithmic parameters that must be set appropriately. Parzen window method is capable of producing reliable PDF estimates with the aid of relatively short data records (Bowman & Azzalini, 1997; Parzen, 1962; Silverman, 1996). Therefore, the associated BER estimate (21) is an accurate one, provided that the kernel variance ρ^2 is chosen appropriately, and hence this approach is capable of approaching the optimal Bayesian performance.

In order to derive a sample-by-sample adaptive algorithm, consider a "single-sample PDF estimate" of $p_y(y_s)$ given by

$$\tilde{p}_y(y_s, k) = \frac{1}{\sqrt{2\pi}\rho} e^{-\frac{(y_s - \text{sgn}(d(k))y_{\text{RBF}}(k))^2}{2\rho^2}}. \quad (26)$$

Conceptually, given this instantaneous PDF "estimate" we have a single-sample BER "estimate" $\tilde{P}_E(\mathbf{w}, k) = Q(\tilde{g}_k(\mathbf{w}))$. Using the instantaneous gradient of

$$\begin{aligned} \nabla \tilde{P}_E(\mathbf{w}, k) = & -\frac{1}{\sqrt{2\pi}\rho} e^{-\frac{y_{\text{RBF}}^2(k)}{2\rho^2}} \text{sgn}(d(k)) \\ & \times \frac{\partial f_{\text{RBF}}(\mathbf{x}(k); \mathbf{w})}{\partial \mathbf{w}} \end{aligned} \quad (27)$$

gives rise to the following stochastic adaptive algorithm

$$\begin{cases} y_{\text{RBF}}(k) = f_{\text{RBF}}(\mathbf{x}(k); \mathbf{w}(k-1)), \\ \mathbf{w}(k) = \mathbf{w}(k-1) + \frac{\mu}{\sqrt{2\pi}\rho} e^{-\frac{y_{\text{RBF}}^2(k)}{2\rho^2}} \text{sgn}(d(k)) \\ \quad \times \frac{\partial f_{\text{RBF}}(\mathbf{x}(k); \mathbf{w}(k-1))}{\partial \mathbf{w}}, \end{cases} \quad (28)$$

which we refer to as the NLBER algorithm. The step size μ and kernel variance ρ^2 should be chosen appropriately to achieve a desired convergence performance, both in terms of convergence speed and steady-state BER misadjustment.

For the symmetrical RBF detector (14) using the Gaussian function (16), the derivatives of the RBF detector's output with respect to the RBF detector's parameters are given by

Table 1

Number of antenna array elements, number of users supported and locations of users in terms of angle of arrival (AOA)

Example 1: $L = 2$ and $M = 4$

Two-element antenna array supporting four users

User i	1	2	3	4
AOA θ	0°	20°	-30°	-45°

Example 2: $L = 3$ and $M = 5$

Three-element antenna array supporting five users

User i	1	2	3	4	5
AOA θ	0°	10°	-17°	15°	20°

Example 3: $L = 4$ and $M = 7$

Four-element antenna array supporting seven users

User i	1	2	3	4	5	6	7
AOA θ	0°	10°	-12°	15°	20°	-18°	17°

$$\left. \begin{aligned}
 \frac{\partial f_{\text{RBF}}}{\partial \alpha_i} &= e^{-\frac{\|\mathbf{x}(k) - \mathbf{c}_i\|^2}{\sigma_i^2}} - e^{-\frac{\|\mathbf{x}(k) + \mathbf{c}_i\|^2}{\sigma_i^2}}, \\
 \frac{\partial f_{\text{RBF}}}{\partial \sigma_i^2} &= \alpha_i \left(e^{-\frac{\|\mathbf{x}(k) - \mathbf{c}_i\|^2}{\sigma_i^2}} \frac{\|\mathbf{x}(k) - \mathbf{c}_i\|^2}{(\sigma_i^2)^2} \right. \\
 &\quad \left. - e^{-\frac{\|\mathbf{x}(k) + \mathbf{c}_i\|^2}{\sigma_i^2}} \frac{\|\mathbf{x}(k) + \mathbf{c}_i\|^2}{(\sigma_i^2)^2} \right), \\
 \frac{\partial f_{\text{RBF}}}{\partial \mathbf{c}_i} &= \alpha_i \left(e^{-\frac{\|\mathbf{x}(k) - \mathbf{c}_i\|^2}{\sigma_i^2}} \frac{\mathbf{x}(k) - \mathbf{c}_i}{\sigma_i^2} \right. \\
 &\quad \left. + e^{-\frac{\|\mathbf{x}(k) + \mathbf{c}_i\|^2}{\sigma_i^2}} \frac{\mathbf{x}(k) + \mathbf{c}_i}{\sigma_i^2} \right),
 \end{aligned} \right\} \quad (29)$$

for $1 \leq i \leq n_c$. Since the number of users M is usually known, the number of RBF units can be set to $n_c \leq N_{sb}$.

Convergence properties of this NLBER algorithm is not well known, although our extensive simulation experience has suggested that it is not too difficult for tuning the two algorithmic parameters, μ and ρ^2 , to achieve a reasonable convergence speed. Furthermore, at the time of writing there exists no theoretical result for analysing the steady-state BER misadjustment of the NLBER algorithm, but in practice we have observed that the steady-state BER misadjustment can often be made very small by carefully tuning the two algorithmic parameters. From (28) it can be seen that the actual adaptive gain is proportional to the ratio of μ to ρ . Therefore, it is the combined effect of the two algorithmic parameters that determines the convergence rate and steady-state BER misadjustment. Increasing the value of ρ^2 will increase the optimal value of μ . The kernel width ρ also influences the accuracy of the PDF estimate and therefore it has an influence to the steady-state BER misadjustment.

4. Simulation study

Three multiple antenna aided beamforming systems were used to demonstrate the efficiency of the proposed adaptive

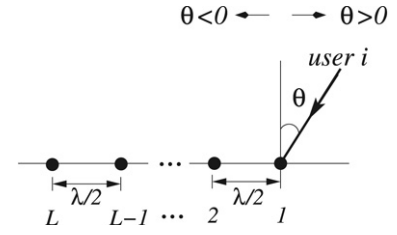


Fig. 1. Geometric structure of the L -element linear antenna array having $\lambda/2$ spacing used in the simulation, where λ is the wavelength.

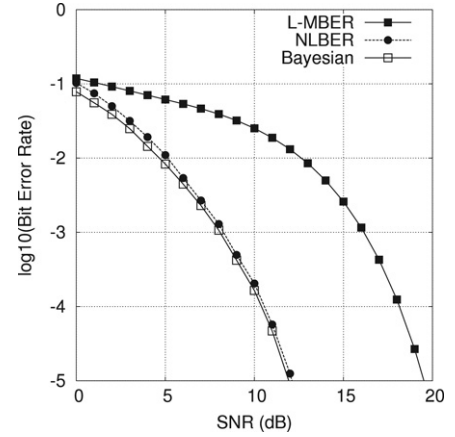


Fig. 2. The desired-user's bit error rate performance in the context of three detectors for the two-element antenna array supporting four users at the angular positions of Table 1. The NLBER-based RBF detector has $n_c = 8$ symmetrical RBF nodes.

NLBER algorithm in the context of the proposed symmetrical RBF detector and to investigate the influence of the two algorithmic parameters, μ and ρ^2 , to the performance of the NLBER algorithm. Fig. 1 shows the angular position of a generic user with respect to the L -element linear antenna array employed in the simulation study. The array element spacing was half of the wavelength. The simulated narrowband channels were $A_i = 1 + j0$, $1 \leq i \leq M$. The desired user and all the interfering users had equal signal power, and therefore we had $\text{SIR}_i = 0$ dB for $2 \leq i \leq M$.

Example 1. A two-element antenna array was designed to support four BPSK signal sources. The users' angular positions are summarized in Table 1. Fig. 2 depicts the BER performance of both the theoretical L-MBER beamformer and the Bayesian detector for the desired user. For this example, the size of the Bayesian detector is specified by the number of symmetrical signal states $N_{sb} = 8$. First, the convergence performance of the NLBER algorithm was investigated. Given a SNR value of 7 dB and a detector size of $n_c = 8$, Fig. 3 shows the learning curve of the NLBER algorithm averaged over 10 independent simulation runs. In Fig. 3, we used the first eight data points as the initial RBF centres $\mathbf{c}_i(0)$, set the initial RBF weights to $\alpha_i(0) = 0.125$ and the initial RBF variances to $\sigma_i^2(0) = \sigma_n^2$, where $1 \leq i \leq n_c = 8$. The step size and kernel variance of the NLBER algorithm (28) were chosen to be $\mu = 0.4$ and $\rho^2 = 10\sigma_n^2$. The learning curve (dashed curve) was the estimated BER $\tilde{P}_E(\mathbf{w}(k))$, calculated using Eq. (21) for each

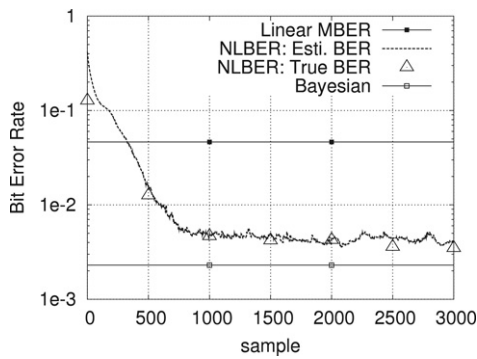


Fig. 3. Learning curve of the NLBER-based RBF detector averaged over 10 runs for the two-element antenna array supporting four users at the angular positions of Table 1, where SNR = 7 dB, the RBF detector has $n_c = 8$ symmetric RBF nodes, and the two algorithmic parameters are set to $\mu = 0.4$ and $\rho^2 = 10\sigma_n^2$.

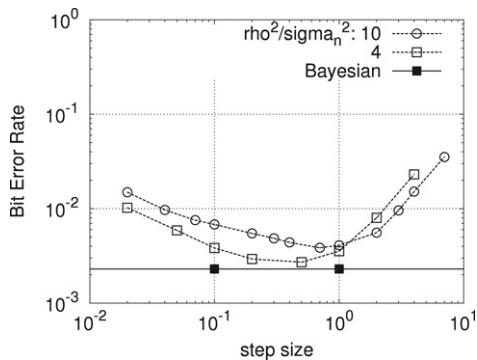


Fig. 4. The influence of the two algorithmic parameters to the steady-state BER performance of the NLBER-based symmetrical RBF detector for the two-element antenna array supporting four users at the angular positions of Table 1, given SNR = 7 dB and $n_c = 8$ symmetrical RBF nodes.

$\mathbf{w}(k)$ in conjunction with a block size of $K = 400$ and a kernel variance of $\tilde{\rho}^2 = \sigma_n^2$. Note that $\tilde{\rho}^2$ was not the kernel variance of the NLBER algorithm and was only used to approximate the BER. In order to check that the estimated BER $P_E(\mathbf{w}(k))$ gave the correct convergence trend, we also calculated the true BER $P_E(\mathbf{w}(k))$ using Monte Carlo simulation for a number of points, shown in Fig. 3 by the triangles. The results of Fig. 3 confirm that the estimated BER correctly indicated the convergence trend and the NLBER algorithm achieved convergence after 800 samples.

The influence of the two algorithmic parameters, μ and ρ^2 , to the steady-state BER performance is illustrated in Fig. 4, under the similar conditions for obtaining Fig. 3. It can be seen that $\rho^2 = 4\sigma_n^2$ gave a better steady-state BER performance than the case of $\rho^2 = 10\sigma_n^2$. However, we observed in the simulation that $\rho^2 = 10\sigma_n^2$ achieved a fast convergence than the case of $\rho^2 = 4\sigma_n^2$. Also from Fig. 4 it can be seen that an appropriate value of μ depends on the value of ρ^2 used. The influence of the number of RBF centres n_c on the performance of the NLBER-based symmetrical RBF detector was studied next. Given SNR = 7 dB and the same initial conditions as before, Fig. 5 illustrates the performance of the NLBER-based detector as a function of model size or the number of RBF centres n_c . It can be seen that for $n_c \geq N_{sb}$ the

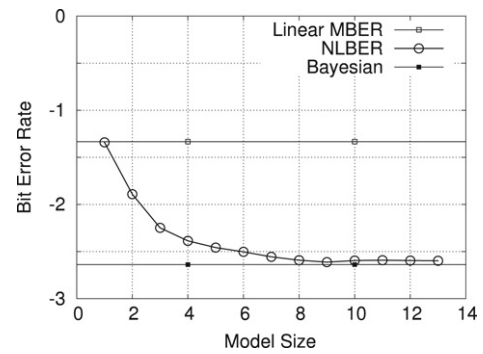


Fig. 5. The influence of the detector's size on the bit error rate performance of the NLBER-based symmetrical RBF detector for the two-element antenna array supporting four users at the angular positions of Table 1, where we have SNR = 7 dB.

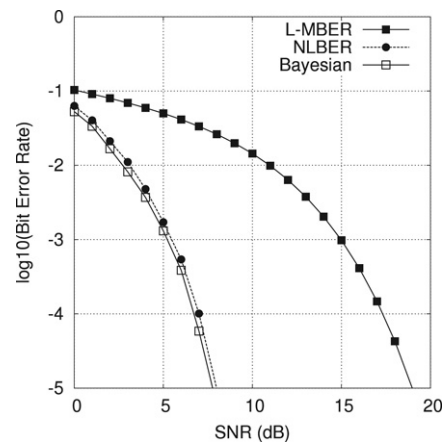


Fig. 6. The desired-user's bit error rate performance in the context of three detectors for the three-element antenna array supporting five users at the angular positions of Table 1. The NLBER-based RBF detector has $n_c = 16$ symmetrical RBF nodes.

symmetrical RBF detector trained by the stochastic NLBER algorithm becomes capable of closely approaching the optimal Bayesian performance. It is also interesting to observe in Fig. 5 that using a single symmetrical RBF node the detector achieves the same performance as the L-MBER solution, since the detector of a single symmetrical RBF node is only capable of constructing a linear decision boundary. For each SNR value, the BER performance of the NLBER-based symmetrical RBF detector having $n_c = 8$ RBF nodes is depicted in Fig. 2, in comparison to the optimal Bayesian performance.

Example 2. The system consisted of a three-element antenna array designed for supporting five BPSK users. The users' angular locations are summarized in Table 1. The BER performance of the two benchmarks, namely those of the L-MBER beamformer and the Bayesian detector, are shown in Fig. 6. The size of the Bayesian detector in this example is $N_{sb} = 16$. The convergence performance of the NLBER algorithm is characterized in Fig. 7, given SNR = 5 dB and $n_c = 16$. Again, the learning curve of Fig. 7 was averaged over 10 runs, and we used the first 16 data points as the initial RBF centres, set all the initial RBF weights to $1/16 \approx 0.06$ and all the initial RBF variances to $9\sigma_n^2$. It was found empirically

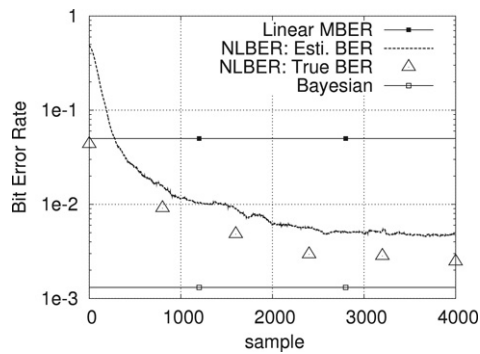


Fig. 7. Learning curve of the NLBER-based RBF detector averaged over 10 runs for the three-element antenna array supporting five users at the angular positions of Table 1, where SNR = 5 dB, the RBF detector has $n_c = 16$ symmetrical RBF nodes, and the two algorithmic parameters are set to $\mu = 0.4$ and $\rho^2 = 4\sigma_n^2$.

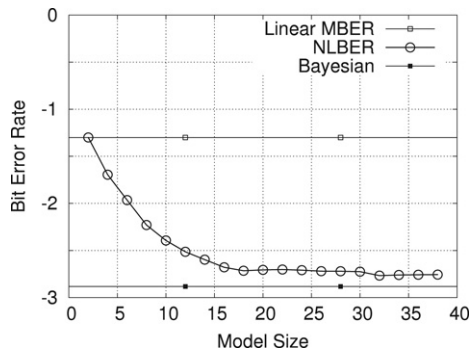


Fig. 8. The influence of the detector's size on the bit error rate performance of the NLBER-based symmetrical RBF detector for the three-element antenna array supporting five users at the angular positions of Table 1, where we have SNR = 5 dB.

that appropriate values for the two algorithmic parameters of the adaptive NLBER algorithm were μ in the range of 0.3–0.5 and ρ^2 in the range of $3\sigma_n^2$ to $5\sigma_n^2$, respectively. The step size $\mu = 0.4$ and kernel variance $\rho^2 = 4\sigma_n^2$ were chosen to obtain the convergence curve of Fig. 7. The block size used for estimating the approximated BER $\tilde{P}_E(\mathbf{w}(k))$ was $K = 800$ in conjunction with a kernel variance of $\tilde{\rho}^2 = \sigma_n^2$. The true BER markers (triangles) in Fig. 7 confirm that the learning curve $\tilde{P}_E(\mathbf{w}(k))$ correctly indicated the convergence trend and the algorithm achieved convergence after 2500 samples of training. Given SNR = 5 dB and the same initial conditions as before, Fig. 8 illustrates the influence of the number of RBF centres n_c on the BER performance of the NLBER-based symmetrical RBF detector. Upon using $n_c = 16$ symmetrical RBF nodes, the performance of the NLBER-based symmetrical RBF detector is compared to those of the other two benchmarks in Fig. 6.

Example 3. A four-element antenna array was used to support seven BPSK users. The users' angular locations are again summarized in Table 1. The BER performance of the L-MBER beamformer and the optimal Bayesian detector are shown in Fig. 9. The size of the Bayesian detector in this example is $N_{sb} = 64$. Fig. 10 shows the convergence performance of the NLBER algorithm averaged over 10 runs, given SNR = 4 dB

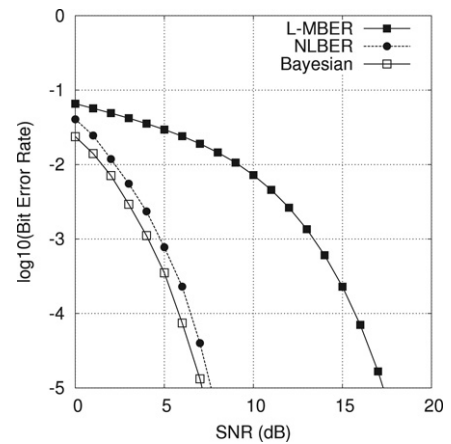


Fig. 9. The desired-user's bit error rate performance in the context of three detectors for the four-element antenna array supporting seven users at the angular positions of Table 1. The NLBER-based RBF detector has $n_c = 60$ symmetrical RBF nodes.

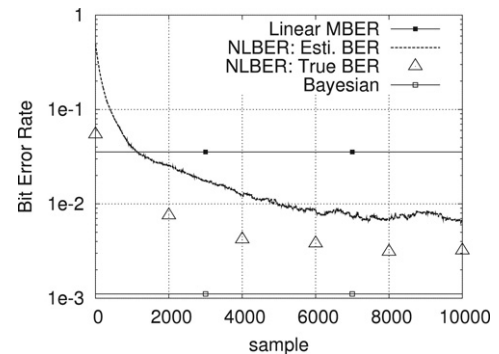


Fig. 10. Learning curve of the NLBER-based RBF detector averaged over 10 runs for the four-element antenna array supporting seven users at the angular positions of Table 1, where SNR = 4 dB, the RBF detector has $n_c = 60$ symmetrical RBF nodes, and the two algorithmic parameters are set to $\mu = 0.5$ and $\rho^2 = \sigma_n^2$.

and $n_c = 60$. In order to obtain the learning curve of Fig. 10, we used the first 60 data points as the initial RBF centres, set all the initial RBF weights to 0.01 and all the initial RBF variances to σ_n^2 . The step size and kernel variance of the adaptive NLBER algorithm (28) were set empirically to be $\mu = 0.5$ and $\rho^2 = \sigma_n^2$. The block size used for estimating the approximated BER $\tilde{P}_E(\mathbf{w}(k))$ of (21) was $K = 2000$ along with a kernel variance of $\tilde{\rho}^2 = \sigma_n^2$. Note that the convergence rate shown in Fig. 10 was reasonable, considering the fact that the number of total adjustable parameters in \mathbf{w} for this example was 600. When using $n_c = 60$ symmetrical RBF nodes, the performance of the NLBER-based symmetrical RBF detector is compared to those of the other two benchmarks in Fig. 9.

5. Conclusions

A novel symmetric RBF network has been proposed for nonlinear detection in beamforming, which is capable of substantially outperforming previous solutions found in the literature in the extremely challenging scenario of supporting almost twice as many users, as the number of antenna elements

in multiple-antenna aided beamforming systems. A powerful adaptive algorithm based on a stochastic approximation of Parzen window density estimation has been derived for training the symmetrical RBF detector. It has been shown using a simulation study that this novel NLBER algorithm is capable of approaching the optimal Bayesian detection performance. The proposed solution is capable of providing an SNR gain in excess of 8 dB against the powerful linear minimum bit error rate benchmark, when supporting four users with the aid of two receive antennas or seven users employing four receive antenna elements. A practical way of applying this NLBER algorithm is to combine it with the block-data-based algorithm for the symmetrical RBF detector, presented in Chen et al. (2007). During the link set up, the block-data-based algorithm of Chen et al. (2007) is used to construct the initial symmetrical RBF detector, while during the communication phase the NLBER algorithm is used to adapt the detector in order to track time-varying channels.

Our future research will focus on the extension of this NLBER-based symmetrical RBF detector to the generic multiple-input multiple-output communication system in the framework of space–time equalisation, where frequency selective channels are encountered. Further work will also be carried out to investigate decision-directed adaptation for the NLBER algorithm in order to shorten the training length and to extend the present results to multi-level modulation schemes.

Acknowledgments

The financial supports of the EU, under the auspices of the Phoenix and Newcom projects, and the EPSRC UK are gratefully acknowledged.

References

- Abend, K., & Fritchman, B. D. (1970). Statistical detection for communication channels with intersymbol interference. *Proceedings of the IEEE*, 58(5), 779–785.
- Aguirre, L. A., Lopes, R. A. M., Amaral, G. F. V., & Letellier, C. (2004). Constraining the topology of neural networks to ensure dynamics with symmetry properties. *Physical Review E*, 69, 026701-1–026701-11.
- Albu, F., & Martinez, D. (1999). The application of support vector machines with Gaussian kernels for overcoming co-channel interference. In *Proc. 9th IEEE int. workshop neural networks for signal processing* (pp. 49–57).
- Bloch, J. S., & Hanzo, L. (2002). *Third generation systems and intelligent wireless networking—smart antennas and adaptive modulation*. Chichester, UK: Wiley.
- Bowman, A. W., & Azzalini, A. (1997). *Applied smoothing techniques for data analysis*. Oxford, UK: Oxford University Press.
- Chen, S., & Mulgrew, B. (1992). Overcoming co-channel interference using an adaptive radial basis function equaliser. *Signal Processing*, 28(1), 91–107.
- Chen, S., Mulgrew, B., & Grant, P. M. (1993). A clustering technique for digital communications channel equalisation using radial basis function networks. *IEEE Transactions on Neural Networks*, 4(4), 570–579.
- Chen, S., McLaughlin, S., Mulgrew, B., & Grant, P. M. (1995). Adaptive Bayesian decision feedback equaliser for dispersive mobile radio channels. *IEEE Transactions on Communications*, 43(5), 1937–1946.
- Chen, S., Mulgrew, B., & Hanzo, L. (2000). Asymptotic Bayesian decision feedback equalizer using a set of hyperplanes. *IEEE Transactions on Signal Processing*, 48(12), 3493–3500.
- Chen, S., Samingan, A. K., & Hanzo, L. (2001). Support vector machine multiuser receiver for DS-CDMA signals in multipath channels. *IEEE Transactions on Neural Networks*, 12(3), 604–611.
- Chen, S., Gunn, S. R., & Harris, C. J. (2001). The relevance vector machine technique for channel equalization application. *IEEE Transactions on Neural Networks*, 12(6), 1529–1532.
- Chen, S., Hanzo, L., & Mulgrew, B. (2001). Decision feedback equalization using multiple-hyperplane partitioning for detecting ISI-corrupted M -ary PAM signals. *IEEE Transactions on Communications*, 49(5), 760–764.
- Chen, S., Hanzo, L., & Wolfgang, A. (2004a). Nonlinear multi-antenna detection methods. *EURASIP Journal on Applied Signal Processing*, 2004(9), 1225–1237.
- Chen, S., Hanzo, L., & Wolfgang, A. (2004b). Kernel-based nonlinear beamforming construction using orthogonal forward selection with Fisher ratio class separability measure. *IEEE Signal Processing Letters*, 11(5), 478–481.
- Chen, S., Ahmad, N. N., & Hanzo, L. (2005). Adaptive minimum bit error rate beamforming. *IEEE Transactions on Wireless Communications*, 4(2), 341–348.
- Chen, S., Hanzo, L., Ahmad, N. N., & Wolfgang, A. (2005). Adaptive minimum bit error rate beamforming assisted receiver for QPSK wireless communication. *Digital Signal Processing*, 15(6), 545–567.
- Chen, S., Du, H.-Q., & Hanzo, L. (2006). Adaptive minimum symbol error rate beamforming assisted receiver for quadrature amplitude modulation systems. In *Proc. VTC2006-Spring* (pp. 2236–2240).
- Chen, S., Wolfgang, A., Harris, C. J., & Hanzo, L. (2007). Symmetric kernel detector for multiple-antenna aided beamforming systems. In *Proc. IJCNN-2007* (pp. 2486–2491).
- Chen, S., Hanzo, L., & Tan, S. (2008). Nonlinear beamforming for multiple-antenna assisted QPSK wireless systems. *ICC 2008*. 2008 (submitted for publication).
- Duda, R. O., & Hart, P. E. (1973). *Pattern classification and scene analysis*. New York: Wiley.
- Espinoza, M., Suykens, J. A. K., & De Moor, B. (2005). Imposing symmetry in least squares support vector machines regression. In *Proc. joint 44th IEEE conf. decision and control, and the european control conf. 2005* (pp. 5716–5721).
- Godara, L. C. (1997a). Applications of antenna arrays to mobile communications, Part I: Performance improvement, feasibility, and system considerations. *Proceedings of the IEEE*, 85(7), 1031–1060.
- Godara, L. C. (1997b). Applications of antenna arrays to mobile communications, Part II: Beam-forming and direction-of-arrival considerations. *Proceedings of the IEEE*, 85(8), 1193–1245.
- Kohno, R. (1998). Spatial and temporal communication theory using adaptive antenna array. *IEEE Personal Communications*, 5(1), 28–35.
- Litva, J., & Lo, T. K. Y. (1996). *Digital beamforming in wireless communications*. London: Artech House.
- Parzen, E. (1962). On estimation of a probability density function and mode. *The Annals of Mathematical Statistics*, 33, 1066–1076.
- Paulraj, A. J., & Papadias, C. B. (1997). Space-time processing for wireless communications. *IEEE Signal Processing Magazine*, 14(6), 49–83.
- Paulraj, A., Nabar, R., & Gore, D. (2003). *Introduction to space–time wireless communications*. Cambridge, UK: Cambridge University Press.
- Paulraj, A. J., Gore, D. A., Nabar, R. U., & Bölcskei, H. (2004). An overview of MIMO communications—A key to gigabit wireless. *Proceedings of the IEEE*, 92(2), 198–218.
- Pérez-Cruz, F., Navia-Vázquez, A., Alarcón-Diana, P. L., & Artés-Rodríguez, A. (2001). SVC-based equalizer for burst TDMA transmissions. *Signal Processing*, 81(8), 1681–1693.
- Sebald, D. J., & Bucklew, J. A. (2000). Support vector machine techniques for nonlinear equalization. *IEEE Transactions on Signal Processing*, 48(11), 3217–3226.
- Silverman, B. W. (1996). *Density estimation*. London: Chapman Hall.
- Soni, R. A., Buehrer, R. M., & Benning, R. D. (2002). Intelligent antenna system for cdma2000. *IEEE Signal Processing Magazine*, 19(4), 54–67.
- Steele, R., & Hanzo, L. (1999). *Mobile radio communications*. Piscataway, NJ: IEEE Press.

- Tse, D. N. C., & Hanly, S. V. (1999). Linear multiuser receivers: Effective interference, effective bandwidth and user capacity. *IEEE Transactions on Information Theory*, 45(2), 641–657.
- Tse, D., & Viswanath, P. (2005). *Fundamentals of wireless communication*. Cambridge, UK: Cambridge University Press.
- Tsoulos, G. V. (1999). Smart antennas for mobile communication systems: Benefits and challenges. *IEE Electronics and Communications Journal*, 11(2), 84–94.
- Tsoulos, G., Beach, M., & McGeehan, J. (1997). Wireless personal communications for the 21st century: European technological advances in adaptive antennas. *IEEE Communications Magazine*, 35(9), 102–109.
- Vandenameele, P., van Der Perre, L., & Engels, M. (2001). *Space division multiple access for wireless local area networks*. Boston: Kluwer Academic Publishers.
- Wells, M. C. (1996). Increasing the capacity of GSM cellular radio using adaptive antennas. *IEE Proceedings on Communications*, 143(5), 304–310.
- Winters, J. H. (1998). Smart antennas for wireless systems. *IEEE Personal Communications*, 5(1), 23–27.
- Winters, J. H., Salz, J., & Gitlin, R. D. (1994). The impact of antenna diversity on the capacity of wireless communication systems. *IEEE Transactions on Communications*, 42(2–4), 1740–1751.
- Wolfgang, A., Chen, S., & Hanzo, L. (2004). Radial basis function network assisted space–time equalisation for dispersive fading environments. *Electronics Letters*, 40(16), 1006–1007.